Title:

Closing the Duration Gap in RVT: The Energetic Duration

Authors:

Rajesh Rupakhety[1]

Víctor M. Hernández-Aguirre[2]

[1] Earthquake Engineering Research Centre, Faculty of Civil and Environmental Engineering, University of Iceland, Austurvegur 2a, 800 Selfoss, Iceland

Email: rajesh@hi.is

[2] Earthquake Engineering Research Centre, Faculty of Civil and Environmental Engineering, University of Iceland, Austurvegur 2a, 800 Selfoss, Iceland

Email: victorh@hi.is

Preprint Statement

This manuscript is a preprint and has not undergone peer review.

The manuscript is currently under review in Soil Dynamics and Earthquake Engineering.

This version is posted on EarthArXiv to ensure transparency, accessibility, and timely dissemination of the research.

The final published version, if accepted, may differ from this preprint.

Date of Preprint Posting:

29 April 2026

Closing the Duration Gap in RVT: The Energetic Duration

Abstract

Duration is a fundamental descriptor of earthquake ground motion, yet it remains ill-defined across engineering seismology, with numerous threshold-based measures adopted for specific applications. This ambiguity has allowed duration to function as a calibration parameter in analyses such as random vibration theory (RVT), where it is often adjusted to match observed response spectra. This paper introduces a new definition based on the participation ratio of the temporal energy distribution, yielding the energetic duration D^*. When applied consistently, D^* provides an objective measure of the quasi-stationary, peak-generating phase of ground motion and resolves the internal consistency problem of RVT. The framework is extended to a rotation-invariant formulation and to a duration spectrum $\mathrm{D}^*_R(T)$, providing a period-dependent duration consistent with oscillator response. The analysis further shows that conventional moment-based estimates of bandwidth and crossing rates are biased under finite-duration conditions, particularly when D/T is small. An empirical correction based on a sinusoidal baseline test, combined with time-domain estimation of zero-crossing rates, is introduced to mitigate these effects, improving the stability of RVT peak-factor calculations and reducing both bias and dispersion of predicted spectral ordinates. The proposed approach provides a physically grounded and analytically consistent definition of duration, clarifies its role within RVT, and supports its integration into ground-motion modelling and seismic hazard analysis.

Keywords: strong motion, duration, random vibration theory, effective duration, response spectra, peak factor

1. Introduction

Earthquake ground motion is transient: it builds, concentrates its energy, and decays over a finite interval of strong shaking that is typically much shorter than the total record duration. This temporal structure plays a central role in engineering applications, from the assessment of cumulative damage and liquefaction potential to the simulation of intensity measures for seismic hazard analysis. Duration has therefore long been recognized as a fundamental descriptor of ground motion, alongside amplitude and frequency content (Bommer and Martínez-Pereira, 1999).

Despite this importance, duration has not been defined in a manner consistent with the analytical frameworks in which it is used. Bommer and Martínez-Pereira (1999) identified approximately thirty definitions, each motivated by specific applications rather than a unifying principle, reflecting the absence of a consistent physical or analytical definition. The most widely adopted measure, significant duration, is defined as the time interval between specified percentiles of cumulative Arias (1970) intensity, most commonly D_{5-95} or D_{5-75}, and has been successfully modelled in terms of magnitude, distance, and site effects (e.g., Afshari and Stewart, 2016). However, the percentile thresholds themselves are conventional rather than derived from general principles.

This ambiguity becomes critical because duration enters explicitly into two central analytical frameworks: Fourier spectral analysis and random vibration theory (RVT). In both, duration is not merely descriptive but directly influences the results, yet its selection is typically implicit and inconsistent.

Computation of the Fourier amplitude spectrum (FAS) requires selecting a time window from the record, which contains pre-event noise, strong motion, and decaying coda. Extending the window into the coda introduces low-amplitude contributions not representative of strong shaking, whereas truncation removes transient energy. In practice, the window is often chosen heuristically, and the resulting FAS implicitly reflects that choice: its energy corresponds exactly to the selected time interval, a dependence that propagates into all subsequent analyses.

In RVT, the expected peak response of a process is expressed in terms of its root-mean-square (RMS) level and a peak factor derived from extreme value theory. Both quantities are computed from spectral moments of the FAS and a duration D, which defines the length of the equivalent stationary process (Boore, 2003). Internal consistency requires that the spectral moments, RMS level, and peak factor all correspond to the same stationary process defined over a common duration D. Because the spectral moments are derived from the FAS, this implies that the FAS itself must be computed over the same time interval that defines D (Ou and Herrmann, 1990; Vanmarcke and Lai, 1980). In practice, however, different duration definitions are often applied at different stages, leading to internally inconsistent formulations and biased response spectral predictions, particularly at long periods.

Efforts to correct these biases have led to a succession of duration modifications. Boore and Joyner (1984) introduced an oscillator "memory" term to account for free vibration beyond the excitation. Liu and Pezeshk (1999) refined this correction, while Boore and Thompson (2015) proposed empirical relationships between excitation and RMS duration based on stochastic simulations. Van Houtte et al. (2018) further showed that the Gaussian assumptions underlying RVT peak factors break down at low oscillator frequencies and suggested using oscillator-based significant duration. While each modification addresses observed discrepancies, they do not resolve the underlying issue.

We argue that the origin of these discrepancies lies not in specific duration models but in the absence of a well-defined duration concept. Because duration lacks a principled definition, it can be specified differently at different stages of analysis, effectively acting as a free parameter that absorbs inconsistencies. This is exemplified by the RVT-optimized duration $\mathrm{D}_{\mathrm{rvto}}$ introduced by Bora et al. (2015), defined as the value that minimizes the misfit between RVT predictions and observed response spectra. Although this approach yields unbiased predictions, its physical interpretation is limited. Van Houtte et al. (2018), noted that $\mathrm{D}_{\mathrm{rvto}}$ lacks clear meaning at low frequencies. Subsequent work related $\mathrm{D}_{\mathrm{rvto}}$ to the zeroth spectral moment m_0 (Kolli and Bora, 2021), but this proportionality follows directly from the defining equation and does not constitute an independent physical result. More fundamentally, a duration calibrated using the observed peak and the peak-factor model cannot provide independent information about either. When model assumptions hold, $\mathrm{D}_{\mathrm{rvto}}$ approximates a meaningful stationary duration; when they do not, it absorbs inconsistencies rather than revealing them.

In practice, duration has become the primary parameter through which discrepancies between RVT predictions and observations are reconciled, while the assumptions underlying the peak-factor formulation are less frequently revisited. Unlike spectral moments, which are uniquely determined by the FAS, or peak-factor models, which are mathematically specified, duration remains underdetermined and can absorb bias without physical accountability.

The central premise of this work is that duration must be defined independently of any model that uses it as an input. Once this independence is enforced, inconsistencies that were previously absorbed into duration become directly observable. We therefore propose a duration measure that satisfies three requirements: (i) operational independence, being computed directly from the signal; (ii) internal consistency, ensuring that FAS and RVT quantities refer to the same process; and (iii) quasi-stationary energy concentration, identifying the time interval over which the signal is most consistent with a

stationary stochastic process. Using this duration measure, we demonstrate that enforcing this consistency substantially reduces bias in RVT-based response spectral predictions.

2. Random vibration theory

Random vibration theory provides a frequency-domain route for estimating the expected peak response of a time-domain process without explicitly simulating multiple time histories. In this section we present a short overview of RVT; more details can be found elsewhere (e.g., Boore, 2003; Van Houtte et al., 2018).

For a zero-mean stationary Gaussian process $x(t)$, the expected peak over a finite duration D is expressed as

$$\mathbb{E}[\max |x(t)|] \approx p\, \sigma_x, \tag{1}$$

where σ_x is the RMS amplitude and p is a peak factor. Thus, the peak response is obtained as

$$Y_{\max,\mathrm{RVT}} = p\, Y_{\mathrm{rms}}. \tag{2}$$

For a process with one-sided power spectral density $S(f)$, the variance is

$$\sigma_x^2 = \int_0^\infty S(f)\, df. \tag{3}$$

However, in common engineering seismology RVT workflows, the process is defined via the FAS X(f) and the duration D, given that $S(f) = |X(f)|^2 / D$. The spectral moments of the FAS are defined as

$$m_k = \int_0^\infty f^k\, |X(f)|^2\, df. \tag{4}$$

The connection between the time-domain RMS level and the frequency-domain representation follows from Parseval's theorem

$$m_0 = \int_0^\infty |X(f)|^2\, df = \int_{\mathrm{window}} x^2(t)\, dt, \tag{5}$$

Thus, m_0 represents the energy of the windowed signal. The RMS amplitude is then

$$Y_{\mathrm{rms}} = \sqrt{m_0/D}. \tag{6}$$

The RMS amplitude, spectral moments, peak-factor parameters, and duration should be evaluated from the same windowed time series to ensure that they refer to the same process.

The zero-crossing and extrema rates are obtained from the spectral moments as

$$f_z = \left(\frac{m_2}{m_0}\right)^{1/2}, f_e = \left(\frac{m_4}{m_2}\right)^{1/2}. \tag{7}$$

The corresponding counts over duration D are $N_z = 2f_zD, N_e = 2f_eD$, where the factor of 2 corresponds to counting both upward and downward crossings/extrema. If moments are instead defined using angular frequency, $\omega = 2\pi f$, the familiar $1/(2\pi)$ factors appear explicitly.

2.1 Cartwright–Longuet-Higgins peak factor

The Cartwright and Longuet-Higgins peak factor (1956; CLH), as written by Boore (2003) is

$$p_{CLH} = \sqrt{2}\int_0^\infty \left[1 - \left(1 - \varepsilon\, e^{-x^2}\right)^{N_e}\right] dx, \tag{8}$$

where x is a dimensionless amplitude variable of integration and the bandwidth factor is

$$\varepsilon = \frac{m_2}{\sqrt{m_0 m_4}} = \frac{N_z}{N_e}. \tag{9}$$

For narrow-band motions ($\varepsilon \to 1$), the response can be approximated as a modulated sinusoid, and the distribution of envelope peaks approaches a Rayleigh form. In contrast, for broadband motions ($\varepsilon \to 0$), the peaks follow a Gaussian distribution. This formulation assumes that local extrema are statistically independent (i.e., Poisson process), an assumption that becomes increasingly restrictive for narrowband or highly correlated processes.

Despite this limitation, the CLH peak-factor formulation has been widely used in engineering applications, largely due to its implementation in the SMSIM stochastic simulation framework (Boore, 2003). More recently, however, there has been increasing adoption of the formulation proposed by Vanmarcke (1975; V75). This transition is reflected in updates to SMSIM, where the Vanmarcke peak factor was incorporated in later versions (Boore and Thompson, 2015).

2.2 Vanmarcke peak factor

The V75 formulation accounts for clumping of crossings and avoids the independent-peak assumption used in the CLH model. The cumulative distribution function of the peak factor is

$$F_x(x) = \left[1 - \exp\left(-\frac{x^2}{2}\right)\right] \exp\left\{-N_z \exp\left(-\frac{x^2}{2}\right) \frac{1-\exp\left[-\sqrt{\frac{\pi}{2}}\delta_e x\right]}{1-\exp\left(-\frac{x^2}{2}\right)}\right\}, \tag{10}$$

where

$$\delta_e = \delta^{\,1+b} \;\; and \;\; \delta = \left(1-\frac{m_1^2}{m_0 m_2}\right)^{1/2}, \tag{11}$$

where δ is the Vanmarcke bandwidth parameter. The expected peak factor is then obtained from the complementary cumulative distribution function,

$$p_{\mathrm{V75}} = \mathbb{E}[x] = \int_0^\infty [1 - F_x(x)]\, dx. \tag{12}$$

In this formulation, N_z controls the number of zero-crossing opportunities over the duration D, while δ controls the degree of bandwidth and peak clustering. The exponent $1 + b$ in Eq. (11) is an empirical adjustment introduced by Vanmarcke to improve the fitting to numerical simulations of a simple oscillator to a Gaussian white-noise.

3. The energetic duration

Ground motion records are nonstationary. Peak factor formulations such as those presented in the previous section are derived for stationary processes and require, as a prerequisite, the identification of a time interval over which the signal can be treated as approximately stationary. The energetic duration D^*, developed in the following sections is proposed as the duration of the most energetically concentrated quasi-stationary segment of the signal.

3.1 Definition

Let $\mathrm{a(t)}$ denote the ground acceleration time history over the full processed record. The energetic duration is defined as:

$$\mathrm{D}^* = \frac{\left(\int \mathrm{a}^2(\mathrm{t})\, \mathrm{dt}\right)^2}{\int \mathrm{a}^4(\mathrm{t})\, \mathrm{dt}}, \tag{13}$$

where both integrals are taken over the full record. This quantity has units of time, is strictly positive, and is amplitude-invariant. The numerator of Eq. (13) is proportional to the square of the Arias intensity. The denominator involves the fourth moment of acceleration, which weights high-amplitude portions of the record disproportionately. Signals with short, intense bursts where the fourth moment is

dominated by a few large values have small D^*. Signals with prolonged moderate shaking where amplitude is spread more uniformly have large D^*. This distinction is exactly what RVT needs: it is the duration of the intense phase that determines the number of statistically effective peak opportunities, not the total span of non-negligible motion.

The window of duration D^* is placed to maximize $\int_{window} a^2\,dt/D^*$, i.e., the mean squared amplitude within the window. This placement is unique for records with a single dominant energy packet and well-defined for records with multiple packets as discussed later. Once the window is identified, all quantities entering RVT are computed from the windowed signal.

3.2 Mathematical interpretation

The definition becomes transparent when written in terms of the normalized energy density

$$w(t) = \frac{a^2(t)}{\int a^2(t)\,dt},\ \int w(t)\,dt = 1.$$

The function $w(t)$ is a probability density describing the temporal distribution of signal energy. In this representation

$$D^* = \frac{1}{\int w^2(t)\,dt}.$$

This is the participation ratio of the energy distribution, a concept used in physics to measure localization (Wegner, 1980). When energy is distributed uniformly over a record of length T, $w(t) = 1/T$ and $D^* = T$. When energy is concentrated in a short burst, $\int w^2 dt$ is large and D^* is small. The Cauchy-Schwarz inequality guarantees $D^* \leq T$ with equality only for a perfectly uniform energy history. The quantity D^* therefore measures how much of the record is energetic. It is not a measure of energy span, but its concentration. Two records with the same total energy and the same record length but different degrees of temporal concentration will have different D^* values.

4. Validation of the energetic duration definition

The proposed energetic duration D^* is intended to represent the effective temporal support of the peak-generating process, rather than an energy span of recorded motion. In this section, the behaviour of D^* is examined using a large set of strong-motion records. The dataset used here consists of 4690 strong-motion records from earthquakes with moment magnitude $M_w \geq 5.0$ and Joyner–Boore distance $R_{JB} \leq 200$ km. The records were obtained from the European Strong-Motion (ESM) database (Lanzano et al., 2021), which provides uniformly processed accelerograms together with associated metadata including magnitude, distance measures, and site parameters. The magnitude–distance distribution of the dataset as well as the computed D^* are shown in Figure 1.

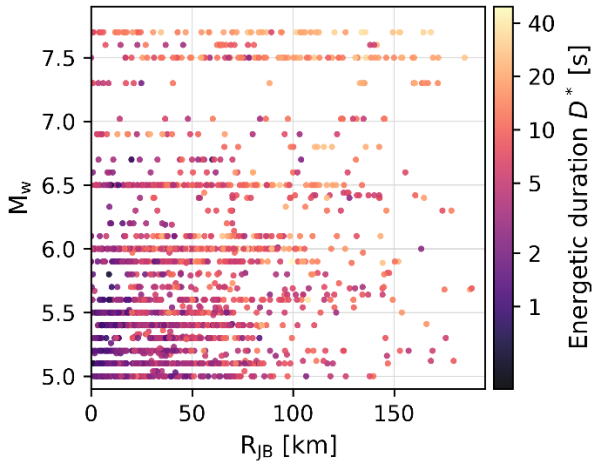

Figure 1. Distribution of records in magnitude–distance space used for the validation of the energetic-duration measure D^*. Marker color indicates the computed energetic duration.

4.1 Example records

The behaviour of the energetic duration D^* is illustrated using representative strong-motion records. Panels (a) and (b) of Figure 2 compare D^*, $D_{5–75}$, and $D_{5–95}$ in both the acceleration time history and the corresponding cumulative energy representation.

For the first record (Figure 2a), D^* is concentrated within the portion of the signal associated with the highest amplitudes and energy content, whereas the percentile-based measures extend beyond this region. The $D_{5–75}$ interval is moderately wider, while $D_{5–95}$ includes a substantial portion of lower-amplitude motion.

This distinction is clarified in Figure 2b. The rapid increase in cumulative energy identifies the interval over which most of the signal energy is released. The energetic duration D^* coincides closely with this interval, whereas the percentile-based durations extend into portions of the record characterized by a markedly lower rate of energy accumulation. Beyond approximately 12 s, the reduced slope of the cumulative energy curve indicates a transition to a lower-intensity regime. In contrast, the slope within the D^* window remains comparatively uniform, consistent with a quasi-stationary segment in a second-moment sense.

A second example (Figure 2c–d) exhibits a more pronounced separation between the duration measures. The record consists of a short interval of strong motion followed by a prolonged, gradually decaying tail. In this case, D^* remains confined to the initial high-energy portion of the record, while the percentile-based durations extend substantially into the coda. As shown in Figure 2d, the majority of the signal energy is accumulated during the initial portion of the record, as indicated by the steep initial increase in cumulative energy. Beyond this interval, the incremental contribution to total energy is small; however, $D_{5–95}$ continues to expand to capture the remaining cumulative energy, resulting in a duration significantly longer than the interval associated with the principal energy release.

This last example illustrates a key limitation of percentile-based duration measures. Because they are defined in terms of cumulative thresholds, they are sensitive to low-energy tails that have little influence on peak response. In contrast, the energetic duration D^* is governed by the temporal concentration of energy and therefore remains anchored to the segment of the record that dominates the peak-generating process. Even for records with extended coda, D^* provides a stable and physically meaningful estimate of the effective quasi-stationary duration relevant to response analysis.

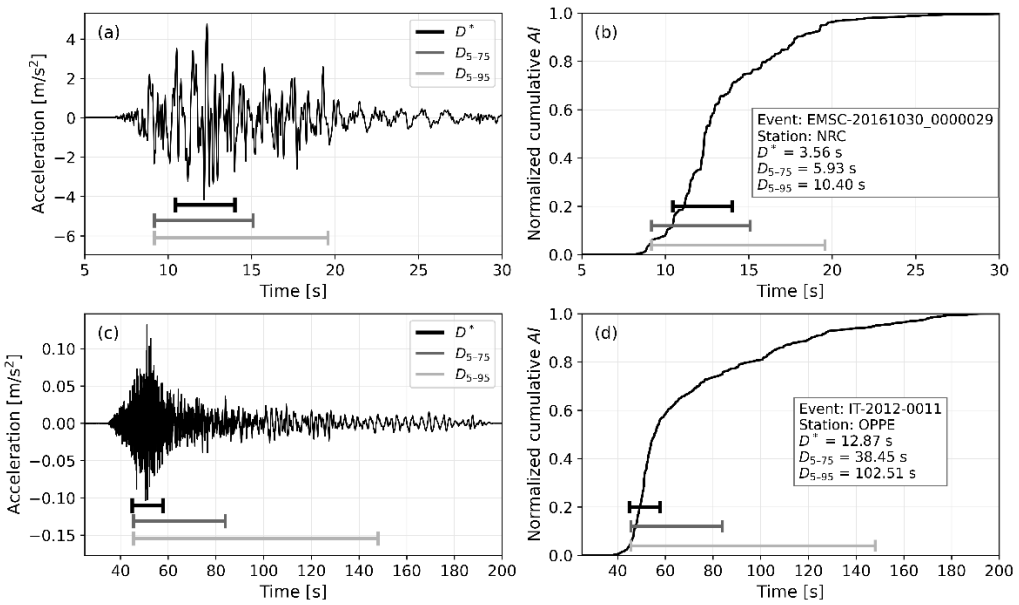

Figure 2. Comparison of D^*, D_{5-75}, and D_{5-95} for a representative record (a-b) and a record with extended low-energy tail (c-d), in terms of acceleration time history (a-c) and normalized cumulative energy (b-d). For the second record the energetic duration D^* remains confined to the early, energy-dominant segment, while percentile-based durations extend into the long, low-energy tail.

4.2 Relationship to significant duration

The relationship between the energetic duration and the significant duration D_{5-95} is summarized in Figure 3. The left panel shows the scatter of D^* versus D_{5-95} on logarithmic axes, together with the equality line and a binned median trend. The two measures are strongly correlated across the dataset (log-space correlation coefficient $r = 0.93$), indicating that both capture the overall temporal scale of ground-motion energy release. However, D^* is systematically smaller, with the median trend lying well below the one-to-one line.

This systematic difference reflects the distinct aspects of the motion that the two measures quantify. The significant duration D_{5-95} represents the interval over which most of the cumulative Arias intensity is accumulated and is therefore sensitive to extended low-amplitude tails. In contrast, D^* is governed by the concentration of energy, emphasizing the time span over which the dominant energy release occurs.

This distinction is further illustrated in the right panel of Figure 3, which shows the ratio D^*/D_{5-95} as a function of D_{5-95}. The ratio is consistently below unity and typically ranges between approximately 0.2 and 0.5, indicating that the effective energetic support of strong-motion energy is substantially shorter than the interval over which cumulative energy continues to grow.

Taken together, these results show that D^* is not a simple rescaling of significant duration, but rather provides a complementary characterization that emphasizes energy concentration rather than cumulative span. At the same time, the strong correlation between D^* and D_{5-95} suggests that predictive models for D^* could be developed using similar explanatory variables (e.g., magnitude, distance, and site conditions), building upon the extensive body of models available for significant duration.

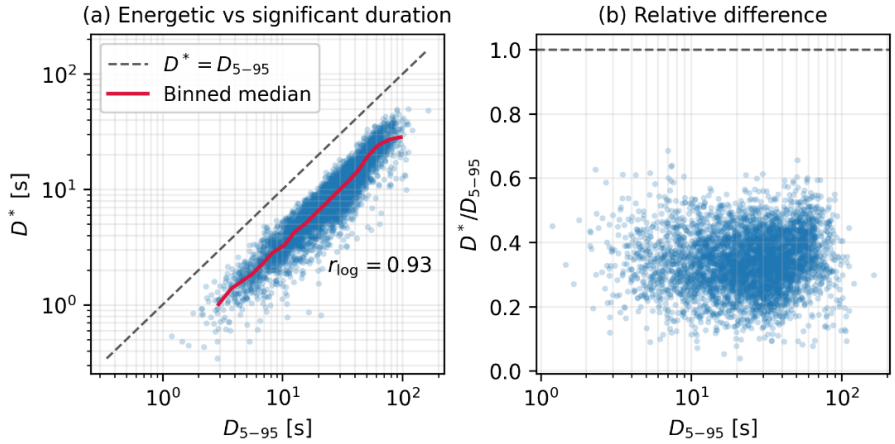

Figure 3. Relationship between energetic duration D^* and significant duration D_{5-95} across the strong-motion dataset. Panel (a) shows D^* versus D_{5-95}; the dashed line indicates equality and the red curve shows the binned median trend. Panel (b) shows the ratio D^*/D_{5-95} as a function of D_{5-95}. The results indicate that D^* is strongly correlated with D_{5-95}.

4.3 Energy concentration within the selected window

To quantify the temporal concentration of energy within a selected window, a measure of window energy density is introduced. For a given time window of duration D, the energy density is defined as

$$\mathrm{q} = \frac{\int_{\text{window}} \mathrm{x}^2(\mathrm{t})\,\mathrm{dt}}{\mathrm{D}}, \tag{14}$$

where $\mathrm{x}(\mathrm{t})$ is the acceleration time history. For zero-mean signals, q is equivalent to the variance of the process within the selected window. For comparison across duration measures, the energy density is normalized by its value computed from the D_{5-95} window. The resulting dimensionless quantity, denoted as $\tilde{\mathrm{q}}$, represents the relative energy concentration of a given window with respect to the conventional D_{5-95} duration, which serves as a baseline.

The distribution of $\tilde{\mathrm{q}}$ across the dataset is shown in Figure 4 for $\mathrm{D}^*$and D_{5-75}. By construction, the energetic duration D^* is associated with a window placement that favours concentration of energy. However, the degree to which this leads to increased energy density is not prescribed by the definition and must be evaluated empirically. The results show that D^* consistently yields substantially higher values of $\tilde{\mathrm{q}}$, with typical values exceeding those of D_{5-95} by a factor of approximately two to three.

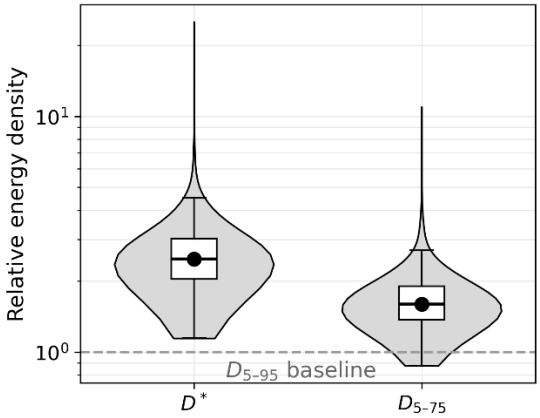

Figure 4. Dataset-wide comparison of energy concentration within the selected window, expressed relative to D_{5-95}. The energetic duration D^* consistently identifies segments with higher variance than percentile-based durations.

The magnitude and consistency of this increase in energy concentration are not trivial consequences of the definition of D^*, but reflect a systematic property of recorded ground motions. By identifying intervals of elevated energy density, the proposed duration D^* provides a measure that is more closely aligned with the characteristics of the peak-generating process.

4.4 Quasi-stationarity within the selected window

The suitability of a duration measure for use in RVT depends not only on its ability to capture the dominant energy of the record, but also on whether the selected time interval can be reasonably approximated as a stationary process. This is a central requirement for the application of RVT if peak factors are derived based on stationary assumptions.

To assess this property, the temporal evolution of energy within each selected window is examined using the normalized cumulative Arias intensity. For a given windowed signal $x_w(t)$ of duration D, the cumulative Arias intensity is defined (up to a constant factor) as the time integral of squared acceleration. The normalized form is expressed as

$$C(\tau) = \frac{\int_{t_0}^{t_0+\tau D} x_w^2(t)\,dt}{\int_{t_0}^{t_0+D} x_w^2(t)\,dt},\ 0 \le \tau \le 1, \tag{15}$$

where τ is the normalized time within the window. This quantity describes the fraction of total energy accumulated as a function of time.

For a process with constant second moment (i.e., stationary variance), the expected rate of energy accumulation is uniform, and the cumulative curve follows a linear trend $C(\tau) = \tau$. Deviations from linearity therefore indicate nonstationary behaviour, with curvature reflecting temporal variations in energy intensity.

Figure 5 presents the median and interquartile range of $C(\tau)$ across the dataset for the different duration measures. The energetic duration D^* yields a cumulative energy curve that is approximately linear over most of the normalized time range, indicating that the selected window corresponds to a segment with relatively stable second-moment properties. In contrast, the $D_{5–95}$ window exhibits pronounced curvature, characterized by rapid initial energy accumulation followed by a gradual flattening, reflecting the inclusion of low-amplitude portions of the record. The $D_{5–75}$ measure shows intermediate behaviour, with reduced but still noticeable deviation from linearity.

These results indicate that, in addition to concentrating energy, D^* identifies a segment of the record that more closely satisfies the assumption of quasi-stationarity in the second-moment sense. This property arises naturally from its focus on the dominant energy-containing portion of the motion, and provides a consistent basis for defining the effective duration of the peak-generating process in RVT.

4.5 Peak containment and multi-packet behaviour

The ability of the selected duration window to contain the absolute peak is examined as a diagnostic of its relation to the peak-generating process. Across the dataset, the energetic duration D^* contains the absolute peak acceleration in most of the records (97%), although not in all cases.

To investigate the cases in which the peak lies outside the D^* window, a subset of records with the largest temporal separation between the peak and the selected window is examined in Figure 6. Some of these examples correspond to multi-segment ruptures such as the 1980 M_w6.8 Irpinia event (IT-1980-0012) and the 2023 M_w7.8 Kahramanmaraş earthquake (INT-20230206-0000008). These records exhibit multiple, temporally separated wave packets, with the absolute peak occurring within a short, high-amplitude transient, while a distinct and often longer-lasting packet contains most of the signal

energy. The energetic duration systematically selects the interval corresponding to the region of sustained energy release.

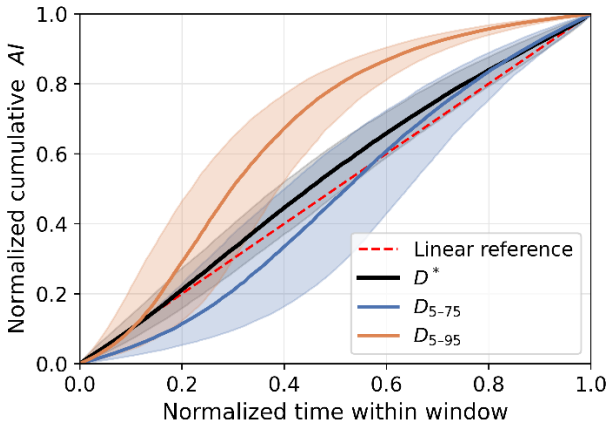

Figure 5. Quasi-stationarity diagnostic based on normalized cumulative Arias intensity within the selected window based on D^*, D_{5-75} and D_{5-95}. A linear trend indicates constant second-moment growth. The energetic duration D^* more closely follows this behaviour, indicating a more nearly quasi-stationary segment.

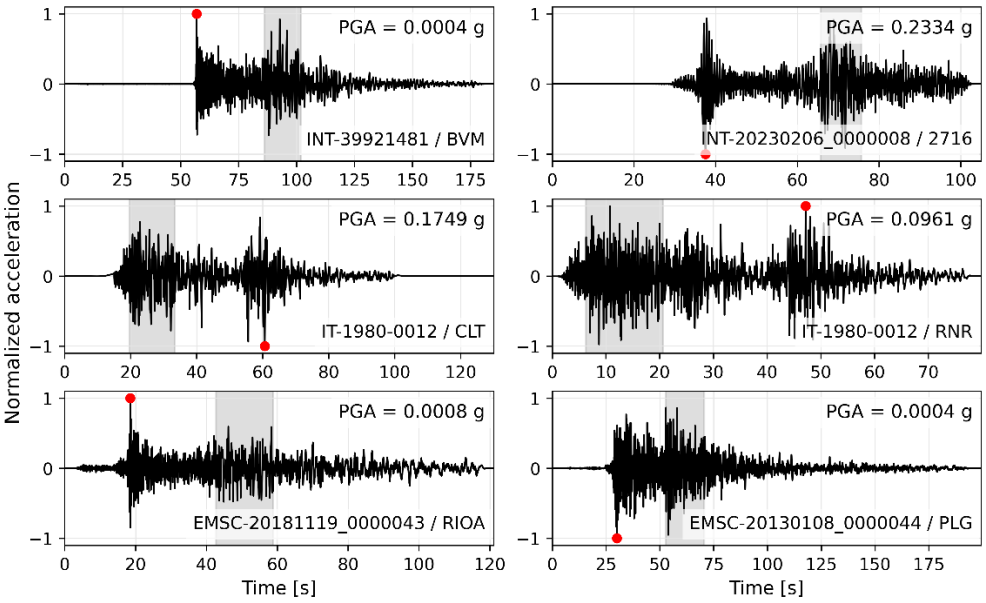

Figure 6. Examples of records in which the absolute peak acceleration lies outside the energetic-duration window D^*. Acceleration time histories (ESM event ID and station code shown in each panel) correspond to the horizontal U component and are normalized by their peak values; the D^* window is shaded and the absolute peak is marked. The records exhibit multiple separated energy packets, with D^* selecting the interval of sustained energy rather than isolated peak excursions.

To further quantify the significance of these cases, the ratio between the maximum absolute acceleration within the D^* window and the global peak of the record is examined for all records in which the peak lies outside the selected window. The resulting distribution, shown in Figure 7, indicates that most of such cases correspond to only minor differences in peak amplitude. The median ratio is approximately 0.92, and a large fraction of the records exhibit ratios exceeding 0.9, demonstrating that the D^* window typically captures a peak of comparable magnitude even when it does not include the absolute maximum.

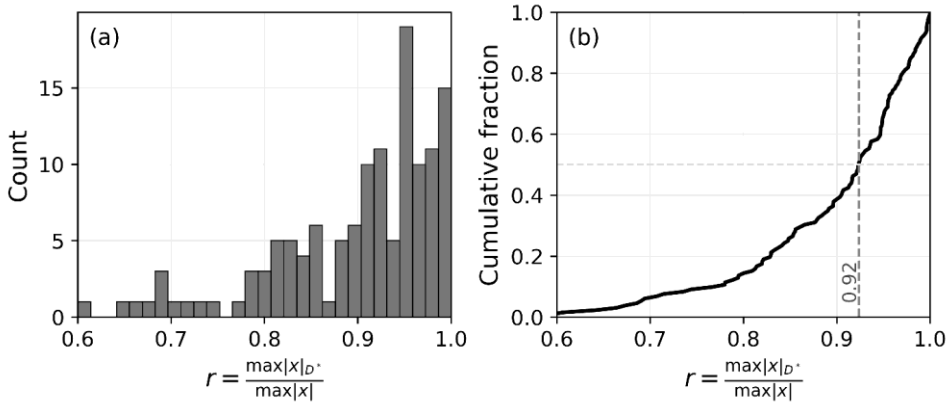

Figure 7. Peak-amplitude ratio $r = max\ |\ x\ |_{D^*}/max|x|$ for records in which the absolute peak lies outside the energetic-duration window. (a) Distribution of r. (b) Empirical cumulative distribution. In most cases, the peak amplitude within the D^* window remains close to the global maximum.

4.6 RVT validation for PGA

In this section, the implications of the energetic duration for peak prediction are evaluated within the RVT framework. For each record, the acceleration time history is restricted to the time interval defined by the duration measure under consideration The extracted segment is tapered using a Tukey window with 10% cosine tapering (5% at each end) to reduce spectral leakage while preserving the effective duration of the signal. All quantities entering the RVT formulation—including the RMS amplitude, spectral moments, and peak factor—are then computed from this windowed signal, ensuring consistency between the temporal support of the data and the assumed stationary process. The predicted peak is obtained as described in Section 2 and compared with the observed peak acceleration within the same window.

Figure 8 summarizes the distributions of residuals, defined as $r = \ln(\mathrm{obs}/\mathrm{pred})$, for the energetic duration $\mathrm{D}^*$and the percentile-based measures $D_{5–75}$ and $D_{5–95}$, using both the CLH and V75 peak-factor formulations. In both cases the energetic duration yields residuals centred near zero, indicating essentially unbiased peak predictions. In contrast, the percentile-based durations exhibit systematic positive bias, corresponding to underprediction of peak amplitudes. The bias increases with window length, with $D_{5–95}$ producing the largest deviations. Furthermore, the dispersion of residuals is reduced when using D^*, as indicated by the narrower interquartile range and steeper empirical cumulative distribution.

The observed behaviour follows directly from the structure of the peak-factor formulation. The peak factor p depends on the number of extrema N_e and/or zero-crossing N_z, which scale linearly with duration. Increasing the duration therefore increases p, reflecting a larger number of statistically effective peak opportunities. However, the predicted peak depends also on the RMS amplitude σ_x (see Eq. 2), which is itself sensitive to the choice of analysis window. Percentile-based durations extend the window into low-amplitude portions of the record that contribute little to the signal variance. As a consequence, the RMS amplitude decreases as the window length increases. Although the peak factor grows with duration, this increase is insufficient to offset the reduction in σ_x. The net effect is therefore a decrease in the predicted peak amplitude, resulting in systematic underprediction.

In contrast, the energetic duration identifies the interval over which the signal is both energetic and approximately stationary in the second-moment sense. As a result, the derived peak factor reflects the actual peak-generating portion of the record. This consistency leads to improved agreement between predicted and observed maxima, both in terms of bias and dispersion.

This demonstrates that duration and variance are not independent quantities in RVT; they are coupled through the definition of the RMS amplitude. The peak scales linearly with the RMS amplitude but only logarithmically with duration through the peak factor. As a result, errors in the estimation of σ_x have a much stronger impact on predicted peak amplitudes than errors in duration. Duration matters in RVT, but primarily through its role in defining a consistent variance–duration pair. If the variance is diluted by including low-energy portions of the record, the resulting peak predictions will be biased regardless of the nominal duration used.

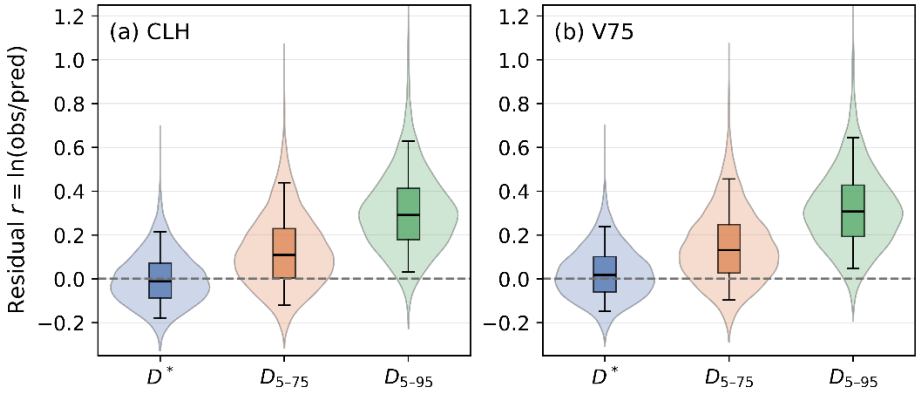

Figure 8. Residual distributions (in log-scale) of RVT PGA predictions for different duration definitions, computed from the peak-factors formulations of (a) Cartwright and Longuet-Higgins (1956; CLH) and (b) Vanmarcke (1975; V75). Violin plots show the full distribution, and the embedded boxplots summarize the median, interquartile range, and 5th–95th percentile range.

5. Rotation-invariant energetic duration

In the analysis of horizontal ground motion, it is common practice to construct rotation-independent measures by evaluating response quantities over all possible orientations of the two horizontal components and summarizing the resulting directional distribution using a statistic such as the median or maximum. This approach underlies widely used measures such as RotD50 and RotD100 (Boore, 2010; Rupakhety and Hernández-Aguirre, 2026a; Rupakhety and Sigbjörnsson, 2013) for response spectra, in which a directional response is computed from rotated components as

$$x_\theta(t) = U(t)\,cos\theta + V(t)\,sin\theta, \tag{16}$$

and the resulting family of values over $\theta \in [0, 180^\circ)$ is reduced to a single representative value.

While this procedure is well suited for amplitude-based response measures, its extension to duration is not straightforward. The energetic duration introduced in this work is not an amplitude quantity but a functional of the signal that depends on both the total energy and its temporal concentration. As such, it reflects properties of the underlying process rather than extrema of directional projections. Applying a percentile operator to a directional family $D^*(\theta)$ therefore lacks a clear physical interpretation, as it combines projections of the motion rather than characterizing the motion itself.

A different approach to orientation dependence was proposed by Rupakhety and Sigbjörnsson (2014), in which strong-motion duration was treated as a random scalar arising from arbitrary sensor orientation, and a representative value was defined through statistical averaging over all possible orientations. For significant duration they show that the duration computed from the horizontal resultant motion provides a close approximation to the mean duration over the directional distribution. This behaviour follows from the fact that cumulative intensity depends only on the integral of squared acceleration, which is additive across components and does not introduce interaction between them.

The present work revisits and extends this concept in the context of energetic duration, which incorporates not only the total energy but also its temporal concentration through second- and fourth-order moments. In contrast to cumulative intensity, this definition introduces nonlinear interaction between components through quartic terms. As a result, the duration computed from the resultant motion is no longer expected to coincide with the mean of the directional durations, since it reflects the temporal support of the combined energy process and may differ systematically from projection-based measures.

A natural way to define a rotation-invariant duration is therefore to base the formulation on invariants of the covariance structure of the horizontal motion. In the horizontal plane, the first invariant of the covariance matrix corresponds to the total variance of the two components, which is equal to the variance of the horizontal resultant acceleration,

$$a_R(t) = \sqrt{U^2(t) + V^2(t)}. \tag{17}$$

This quantity is independent of the orientation of the coordinate system and represents the instantaneous magnitude of the horizontal acceleration vector. The rotation-invariant energetic duration is then defined by applying the same concentration-based formulation to the resultant,

$$D_R^* = \frac{\left(\int a_R^2(t)\,dt\right)^2}{\int a_R^4(t)\,dt}. \tag{18}$$

The associated time window is obtained, as before, by selecting the interval of length D_R^* that maximizes the integrated squared amplitude of $a_R(t)$, and is then applied consistently to both horizontal components.

The relation between the rotation-invariant duration and the directional duration field can be understood from the geometry of horizontal projections. For each instant of time, the rotated component may be written as

$$x_\theta(t) = a_R(t)cos\,(\theta - \phi(t)), \tag{19}$$

where $\phi(t)$ is the instantaneous orientation of the horizontal acceleration vector. It follows that the median over orientation of the absolute directional amplitude satisfies

$$median_\theta \mid x_\theta(t) \mid = \frac{a_R(t)}{\sqrt{2}}, \tag{20}$$

so that the resultant amplitude is exactly $\sqrt{2}$ times the median directional amplitude at each instant of time. This identity is purely geometric and reflects the structure of projections in two dimensions.

Although the energetic duration is a nonlinear functional of the time history, this pointwise geometric relation carries over in an approximate sense to the duration measure. The distribution of the ratio $D_R^*/median_\theta D^*(\theta)$ is shown in Figure 9. The values are tightly clustered around $\sqrt{2}$, with small dispersion, indicating that the rotation-invariant energetic duration is approximately $\sqrt{2}$ times the median directional duration. The slight systematic deviation from $\sqrt{2}$ reflects the nonlinear dependence of duration on the temporal concentration of energy. When energetic contributions from the two components are not perfectly synchronized in time, their combination leads to a broader temporal support of the squared signal, reducing concentration and increasing the duration. Conversely, when the energy is strongly aligned, a single directional projection may capture most of the motion, and the resultant duration approaches the directional values.

These results demonstrate that the rotation-invariant energetic duration provides a consistent and physically meaningful measure of the temporal support of horizontal ground motion. By construction, it is independent of sensor orientation and captures the combined energy release of the vector signal,

while remaining closely related to the directional duration field through simple geometric considerations.

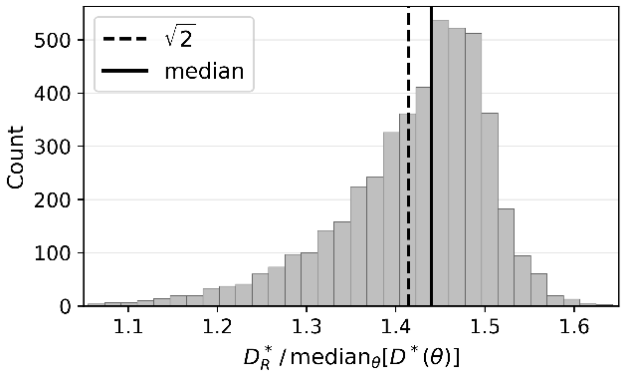

Figure 9. Distribution of the ratio $D_R^*/median_\theta[D^*(\theta)]$ for the dataset. The values are tightly clustered around $\sqrt{2}$, indicating that the rotation-invariant energetic duration is approximately $\sqrt{2}$ times the median directional duration.

5.1 Rotation-invariant duration in RVT predictions

Having established a rotation-invariant definition of energetic duration, its implications RVT predictions are now examined. The time window defined by the resultant-based duration D_R^* is applied consistently to both horizontal components, and RVT predictions are performed separately on each component using the same procedure as in the preceding section. In this way, the dependence of the analysis window on sensor orientation is removed.

The resulting residuals are shown in Figure 10. The distributions for the two components are similar in both bias and dispersion, confirming the consistency of the approach. A small increase in bias is observed relative to the use of component-specific energetic duration, but the overall level of accuracy remains comparable. This behaviour reflects the fact that the rotation-invariant window is defined from the combined energy of both components, rather than being individually optimized for each projection. As a result, the window may not coincide exactly with the optimal interval for a given component. Nevertheless, the use of a common window ensures that both components are evaluated over the same physically meaningful interval representing the total energy release of the horizontal motion.

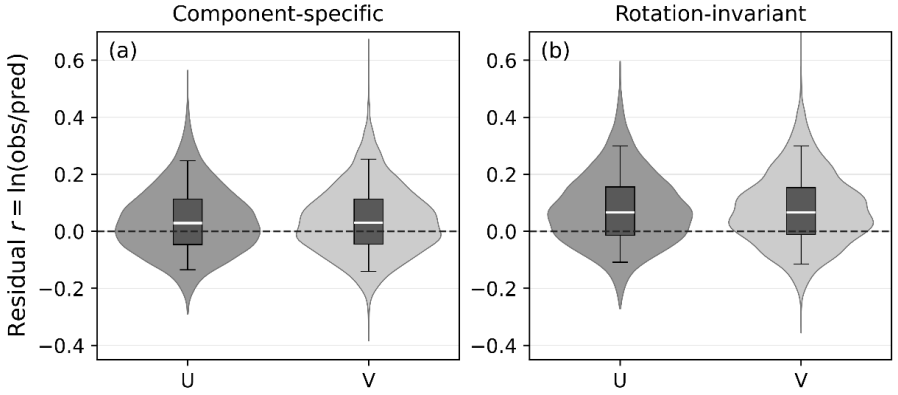

Figure 10. Residuals of RVT PGA predictions from the peak-factor V75 for the two horizontal components using (a) component-specific energetic-duration windows and (b) the rotation-invariant window defined from the horizontal resultant. The invariant window yields similar distributions with a modest increase in bias relative to component-specific windows.

6. The Duration Spectrum

Response spectra encode how oscillator dynamics transform ground-motion amplitude in a period-dependent manner. The same logic applies to temporal support. Once duration is treated as an intrinsic property of a process rather than as an auxiliary record descriptor, the response of a linear oscillator must possess its own duration, and that duration will, in general, depend on oscillator period.

This point has been recognised, in different forms, throughout the literature. Duration is not merely a descriptive characteristic of the input motion: it enters the calculation of the rms response and the peak factor, and therefore directly affects the predicted response spectrum. Historically, this issue has often been handled by introducing a duration associated with the excitation together with an empirical modification or extension intended to represent the longer persistence of oscillator response (Boore and Thompson, 2015). More recent work has moved the discussion closer to the response itself. Van Houtte et al. (2018) argue that, for predicting response spectra, the relevant duration should be linked to the oscillator response rather than to the ground motion, and they show that significant oscillator duration provides a more appropriate RVT input than ground-motion duration. At the same time, they demonstrate that low-frequency oscillator response violates the Gaussian assumptions underlying classical RVT, so that RVT-optimized durations lose a clear physical interpretation in that regime.

The present work is aligned with the response-based motivation of these studies but differs from them in a fundamental way. We do not seek an alternative duration correction or an optimized duration chosen to improve RVT performance. Instead, we extend the energetic duration introduced for ground motion directly to oscillator response. The resulting duration is the same mathematical object applied to a different process. Because the oscillator response changes with period, the resulting duration is necessarily period dependent. This naturally leads to a duration spectrum.

6.1 Definition of the duration spectrum

Let $a_{p,U}(t;T,\xi)$ and $a_{p,V}(t;T,\xi)$ denote the pseudo-acceleration response histories of the two horizontal components for oscillator period T and damping ratio ξ. Consistent with the rotation-invariant treatment developed in Section 5, the resultant oscillator response is defined as

$$a_{p,R}(t;T,\xi) = \sqrt{a_{p,U}^2(t;T,\xi) + a_{p,V}^2(t;T,\xi)}. \tag{21}$$

The energetic duration spectrum is then defined by applying the same moment-ratio functional used for the input motion to the resultant response process:

$$D_R^*(T,\xi) = \frac{\left(\int a_{p,R}^2(t;T,\xi)\,dt\right)^2}{\int a_{p,R}^4(t;T,\xi)\,dt}. \tag{22}$$

This quantity represents the effective temporal support of the total horizontal oscillator response energy. Because it is constructed from the resultant response it is invariant to the orientation of the recorded horizontal axes.

Figure 11 shows the median ± one standard deviation of the duration spectra computed from the whole dataset, with damping ratio of 5% of the critical one. The duration spectrum has two anchoring properties. As $T \to 0$, pseudo-acceleration converges to ground acceleration and therefore $D_R^*(T) \to D_R^*$, the rotation-invariant ground-motion energetic duration. This is the exact temporal analogue of the short-period limit of the response spectrum. At intermediate periods, resonance and oscillator memory redistribute response energy over a longer time interval and $D_R^*(T)$ increases above D_R^*. At long periods the growth slows and $D_R^*(T)$ approaches a broad plateau, reflecting the transition from cycle-resolved response to envelope-controlled behaviour. The full empirical characterisation of the

duration spectrum, including predictive models and comparison with existing duration measures, is the subject of ongoing work.

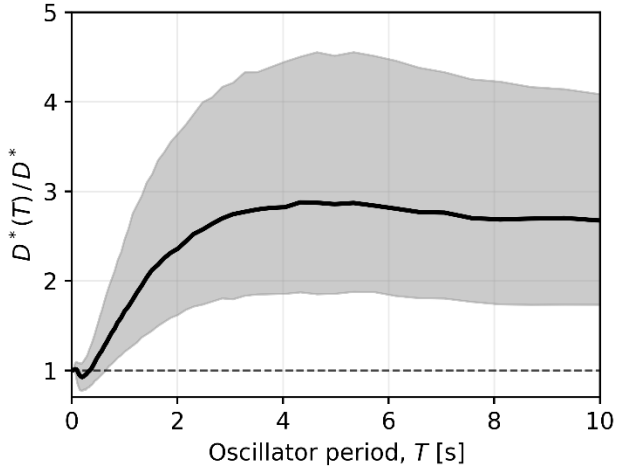

Figure 11. Median ± one standard deviation of the duration spectra computed for the whole dataset, with damping ratio of 5% of the critical one.

7. RVT predictions for spectral response

The duration spectrum provides a well-defined and operationally independent duration input to RVT at each oscillator period. When $D_R^*(T)$ is used together with spectral moments computed from the same windowed oscillator response, the internal consistency requirement is satisfied by construction: the RMS amplitude, peak factor, and duration all refer to the same process over an identical time interval.

A practical limitation arises, however, in the estimation of higher-order spectral moments from finite-duration signals. In particular, the second- and fourth-order moments, m_2 and m_4, are sensitive to spectral leakage and windowing effects. For short windows, these effects artificially inflate the high-frequency content of the spectrum, leading to overestimation of derived quantities. Consequently, the zero-crossing and extrema rates estimated from Eq. (7) are biased high, resulting in inflated values of N_z and N_e. Similarly, bandwidth measures such as δ (Eq. 11) are overestimated, particularly when the ratio D/T is small.

Figure 12 illustrates this behaviour. Panel (a) shows the bandwidth estimated from spectral moments of the pseudo-spectral response (ξ=5%) as a function of $D^*(\mathrm{T})/T$. For large values of $D^*(\mathrm{T})/T$, corresponding primarily to very short periods (T<0.1 s), the response approaches the input acceleration and the bandwidth estimates converge to theoretical values for broadband processes (0.5–0.67 for white-noise and Kanai–Tajimi models; Vanmarcke, 1976). For intermediate values $10 < D^*(\mathrm{T})/T < 40$, the bandwidth decreases towards values consistent with the response of a lightly damped SDOF system (approximately 0.25 for ξ=5%). In contrast, for $D^*(\mathrm{T})/T < 10$, corresponding to long periods, δ increases systematically, even for signals that are nominally narrowband. This trend reflects artificial spectral broadening caused by finite windowing, which becomes dominant when the observation window contains only a few oscillation cycles.

Panel (b) shows the corresponding N_z estimated from spectral moments. The results are compared with the reference relation $N_z = 2D^*(\mathrm{T})/T$, representing the expected behaviour for a narrowband steady-state oscillator response. While the moment-based estimates are broadly consistent with this relation for intermediate $D^*(T)/T$, they deviate systematically at both ends of the range: they are slightly underestimated at very short periods and increasingly overestimated at long periods. The latter

effect is a direct consequence of the inflation of m_2, which increases the apparent zero-crossing rate. This is confirmed in Figure 13, which shows the ratio between zero-crossing counts obtained directly in the time domain and those derived from spectral moments.

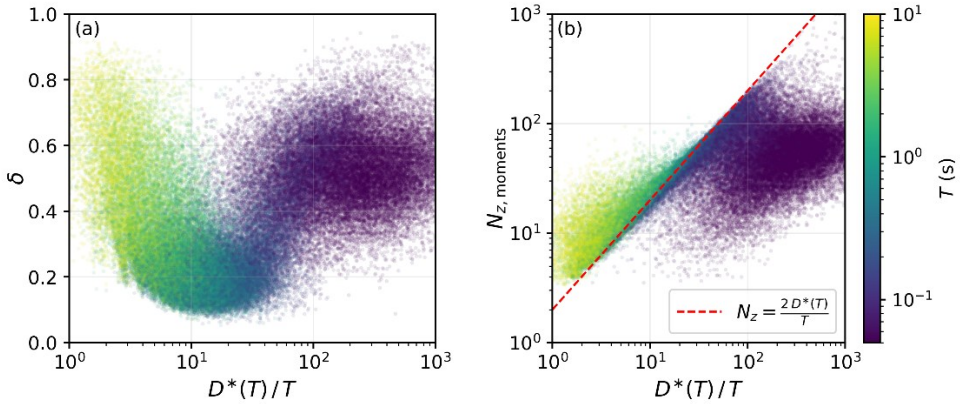

Figure 12. Scatter plots illustrating the effect of finite-duration bias on spectral estimates as a function of D/T. (a) Estimated bandwidth δobtained from spectral moments, showing systematic inflation at low $D^*(T)/T$. (b) Estimated number of zero crossings N_z derived from spectral moments, compared with the reference relation $N_z = 2D^*(T)/T$ (dashed line), which represents the expected value for a narrowband steady-state oscillator response.

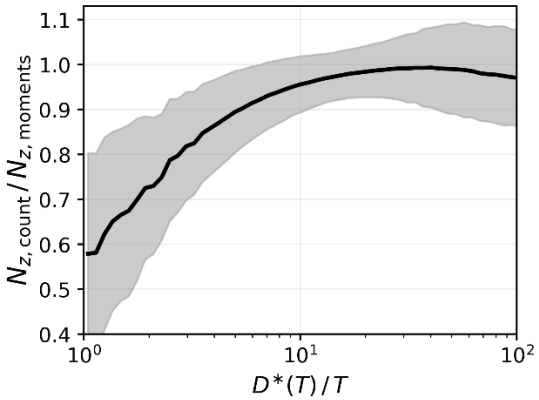

Figure 13. Median ± one standard deviation of the ratio of N_z obtained directly from the count of zero-crossing in the time domain with respect to N_z derived from spectral moments.

These biases have direct implications for peak-factor formulations. The CLH formulation depends on both the extrema count N_e and the bandwidth parameter ε, which rely on accurate estimation of higher-order moments. Finite-duration effects therefore introduce compounded errors in both quantities, leading to unstable and biased peak-factor estimates, particularly at long periods where D/T is small. For this reason, the CLH formulation is not used in the subsequent analyses, and the Vanmarcke formulation is adopted instead, as it relies only on lower-order moments.

The inflation of δ can be illustrated using a simple baseline test. For a pure sinusoidal signal, the true bandwidth is zero. However, when the signal is truncated to a finite window and tapered, the estimated bandwidth becomes nonzero and increases systematically as D/T decreases (Figure 14a). This reflects the fundamental limitation imposed by finite-duration observations: the spectral resolution is bounded below by $1/D$, leading to artificial broadening of otherwise narrowband signals. Consequently, moment-based estimates of crossing rates and bandwidth become unreliable for D/T<10, which is the case for most intermediate and long periods.

This limitation is not merely numerical but statistical. RVT predicts the expected maximum over an ensemble of realizations, whereas observations correspond to a single realization. For a process of duration D and dominant period T, the number of statistically independent cycles is $\mathrm{N_{eff}} \approx 4\pi\xi \mathrm{D}^*/\mathrm{T}$ (Rupakhety and Hernández-Aguirre, 2026b), leading to a coefficient of variation $\mathrm{CV}(\sigma^2) = \sqrt{2/\mathrm{N_{eff}}}$. At long periods, N_{eff} approaches unity, implying that variance estimates—and therefore spectral moments—are inherently unstable. This uncertainty is irreducible and cannot be eliminated by model refinement.

To mitigate the systematic inflation of bandwidth, an empirical correction is introduced based on the sinusoidal baseline test. The correction defines an effective bandwidth δ_{eff} by subtracting a D/T-dependent floor δ_{cor} from the raw estimate δ, with a smooth amplitude-dependent modulation:

$$\delta_{\mathrm{eff}} = \delta - \delta_{\mathrm{cor}}, \quad \delta_{\mathrm{cor}} = \left(\frac{D}{T}\right)^{-1.1}\left(1-e^{-\frac{D/T}{4}}\right)\left[1+\tanh\left(\frac{\delta-0.4}{0.4}\right)\right], \tag{23}$$

Figure 14b shows the median and median ±one standard deviation of δ_{cor} across the dataset as a function of $D^*(\mathrm{T})/T$. The correction effectively removes the spurious increase in bandwidth at low $D^*(T)/T$, while leaving estimates largely unchanged for $D^*(T)/T > 10$.

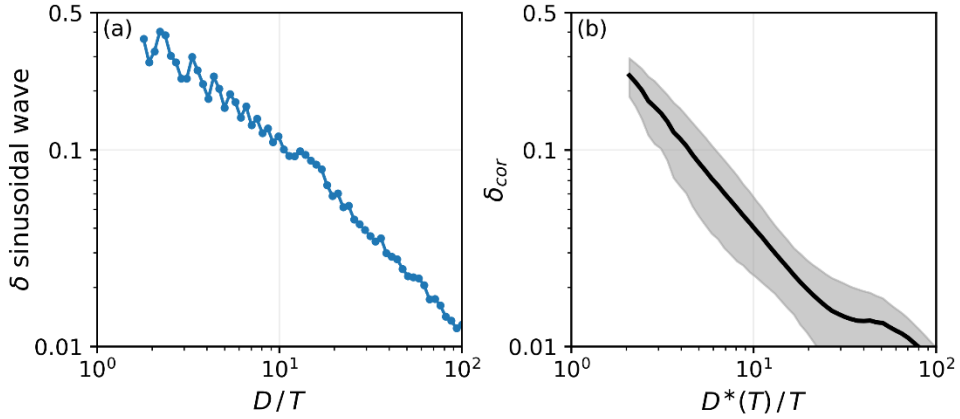

Figure 14. (a) Bandwidth estimates obtained from a finite-duration sinusoidal signal as a function of D/T. Although the true bandwidth is zero, the estimated bandwidth increases systematically as D/T decreases due to spectral leakage and limited frequency resolution. (b) Median and median ±one standard deviation of the bandwidth correction δ_{cor} (see Eq. 23) across the dataset as a function of $D^*(T)/T$.

Figure 15 summarizes the performance of the RVT predictions across the full oscillator period range for three cases, in terms of the median residual $r = \ln(\mathrm{obs/pred})$. Only signals with $D^*(\mathrm{T})/T \geq 2$ are considered. In Case 1, peak factors are computed directly from moment-based estimates using the resultant window. In Case 2, the corrected bandwidth δ_{eff}, time-domain N_z counts, and a modified coefficient $b = 0.15$ (in Eq. 11) are used. Case 3 differs from Case 2 only in that the energetic window is defined separately for each component rather than from the resultant.

Case 1 exhibits a small bias at short periods due to the use of the resultant window and a pronounced overprediction at long periods, consistent with the inflation of bandwidth and crossing rates. In Case 2, the correction reduces this trend, yielding a median residual that is approximately constant with period, although a residual bias remains due to window inconsistency. In Case 3, the bias is effectively removed, with residuals centred near zero across the full period range. The interquartile range (IQR), shown as a shaded band for Case 3, remains approximately constant with period, indicating that both bias and dispersion are controlled when spectral moment corrections and consistent windowing are applied simultaneously.

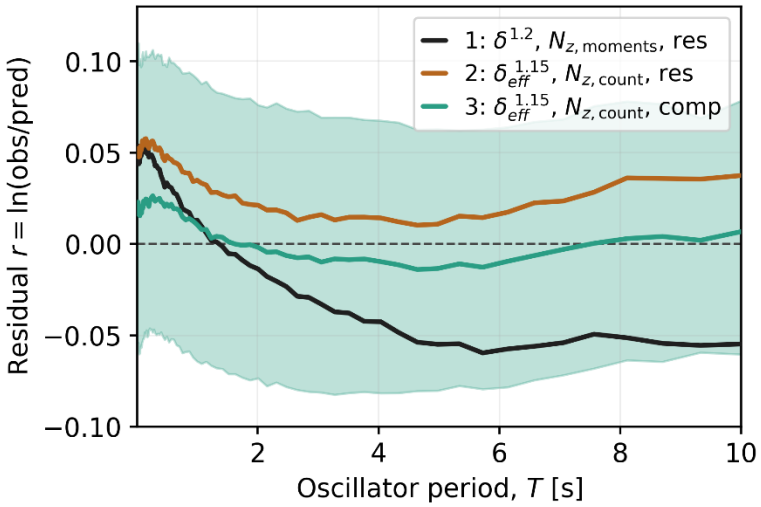

Figure 15. Median residuals $r = ln\ (obs/pred)$ of RVT-predicted spectral acceleration versus oscillator period for three cases. The shaded band shows the interquartile range (25th–75th percentiles) for Case 3. Case 3 achieves near-zero bias across periods, while Cases 1–2 exhibit systematic deviations.

8. Discussion and Conclusions

Duration has occupied a paradoxical position in earthquake ground-motion analysis for decades. It is universally recognised as a fundamental descriptor of shaking, yet it has not been rigorously defined for the purposes to which it is most often applied. In this vacuum, duration has effectively functioned as a free parameter: sufficiently ambiguous that different values can be used at different stages of analysis without apparent contradiction, and sufficiently flexible that it can absorb errors from other components of the RVT framework without physical accountability. This issue is not unique to RVT, but reflects a broader lack of a well-defined, model-independent definition of duration across engineering seismology.

This paper proposes a definition that closes this gap. The energetic duration D^* is defined as the participation ratio of the temporal energy distribution. It requires no threshold, no percentile, and no reference to any downstream model. Instead, it identifies the most energetically concentrated, quasi-stationary segment of the motion. Duration is thereby endowed with a physically interpretable and operationally independent meaning.

For records containing multiple energy packets with different frequency content, the energetic window selection criterion may not always identify the portion of the record most relevant for all applications. Its suitability for problems in which the full span of shaking is critical—such as cumulative damage, liquefaction potential, or fatigue—requires separate evaluation. For records characterised by a short, intense burst followed by a long low-amplitude coda, D^* is substantially shorter than $D_{5–95}$ or $D_{5–75}$. This behaviour is not a deficiency, but rather reflects the fact that the quasi-stationary, peak-generating phase is short, and that extending the analysis window into the coda reduces variance without increasing the number of statistically independent peak opportunities. Whether the coda contributes meaningfully to engineering demand depends on the application, and the duration measure should be selected accordingly.

The relationship between D^* and the significant-duration $D_{5–95}$ provides further insight. Although the two are strongly correlated, D^* is systematically shorter, reflecting its focus on the concentration of energy rather than its cumulative extent. This distinction is critical for RVT, where the relevant duration is that of the peak-generating process, not the full envelope of weak motion. At the same time, the

strong correlation suggests that predictive models for D^* could be developed using similar explanatory variables (e.g., magnitude, distance, and site conditions), providing a practical pathway for integration into hazard analysis workflows.

Because the energetic duration defines a quasi-stationary segment, it has immediate consequences for RVT. When used consistently—i.e., when the same window is used to compute the FAS, spectral moments, RMS amplitude, and peak factor—it enforces internal consistency by construction. The near-zero bias observed in PGA predictions across 4690 records demonstrates that inconsistencies in duration usage were a primary source of error in conventional RVT implementations, and that D^* provides a consistent resolution.

The rotation-invariant extension D_R^* and the associated duration spectrum $\mathrm{D}_R^*(T)$ extend this framework naturally. The results show that the use of a common analysis window for both horizontal components introduces only a minor bias for individual-component predictions. The duration spectrum may be interpreted as the temporal analogue of the response spectrum: it is correctly anchored at short periods, reflects the resonance and ring-down behaviour of oscillator response, and provides a physically consistent duration input to RVT at each oscillator period.

The analysis also highlights a fundamental limitation associated with finite-duration signals. Estimation of higher-order spectral moments from short windows is inherently unstable due to spectral leakage and limited frequency resolution. This leads to systematic inflation of bandwidth and crossing-rate estimates, particularly at long oscillator periods where D^*/T is small. These effects propagate directly into peak-factor formulations, rendering approaches such as the CLH model unreliable in this regime. This limitation is not merely numerical but statistical: for long-period oscillators, the number of effectively independent cycles available within a single record is small, and the variance of spectral estimates is correspondingly large. This uncertainty is irreducible and represents a fundamental constraint on single-record RVT applications.

To address this issue, an empirical correction to the bandwidth was introduced, supported by a baseline sinusoidal test that isolates finite-window effects. In combination with time-domain estimation of zero-crossing counts, this correction stabilizes the inputs to the Vanmarcke peak-factor formulation. The results show that these modifications significantly reduce both bias and dispersion of RVT predictions, particularly at intermediate and long periods where conventional implementations perform poorly. Because the analysis is restricted to a quasi-stationary window, the need for explicitly non-stationary peak-factor formulations (e.g., Corotis et al., 1972) is reduced.

A notable outcome is the good performance of RVT at long periods, where the energetic window is often dominated by the ring-down phase of the oscillator response. In this regime, the motion approaches a decaying sinusoid, and successive peaks are strongly correlated and controlled by damping rather than by stochastic excitation. This behaviour violates the assumptions underlying Gaussian peak-factor models, as also noted by Van Houtte et al. (2018). The satisfactory performance observed here suggests that, despite these violations, the combined effects of consistent windowing, corrected bandwidth, and appropriate crossing-rate estimation compensate for the departure from idealised assumptions. However, this apparent agreement should not be interpreted as validation of the underlying stochastic model in this regime, but rather as a practical approximation whose limits require further investigation.

Several limitations should be noted. First, the present study focuses on pseudo-spectral acceleration and lightly damped oscillators; extension to other intensity measures and damping levels should be examined. Second, the empirical bandwidth correction, while physically motivated, may require further refinements. Third, the RVT validation presented here is based on FAS derived from windowed acceleration time histories, whereas in seismic hazard applications the FAS is typically obtained from

seismological source–path–site models. For D^* to retain its internal consistency in such applications, it should be coupled with FAS models that are explicitly defined over the same energetic window.

Despite these limitations, the results demonstrate that duration can be defined in a manner that is both physically meaningful and analytically consistent. By replacing an ambiguous parameter with a well-defined quantity, the proposed framework clarifies the role of duration in RVT and separates issues of model consistency from intrinsic uncertainty. More broadly, the concept of energetic duration provides a basis for re-examining the role of duration in other areas, where similar inconsistencies may exist.

In this sense, the contribution of this work is not only methodological but conceptual: it shows that duration need not be an adjustable parameter, but can instead be treated as a measurable property of the signal with a clear physical and statistical interpretation.

References

Afshari, K., Stewart, J.P., 2016. Physically Parameterized Prediction Equations for Significant Duration in Active Crustal Regions. Earthq. Spectra 32, 2057–2081. https://doi.org/10.1193/063015EQS106M

Arias, A., 1970. Measure of earthquake intensity. Seism. Des. Nucl. Plants 438–483.

Bommer, J.J., Martínez-Pereira, A., 1999. The effective duration of earthquake strong motion. J. Earthq. Eng. 03, 127–172. https://doi.org/10.1142/S1363246999000077

Boore, D.M., 2010. Orientation-independent, nongeometric-mean measures of seismic intensity from two horizontal components of motion. Bull. Seismol. Soc. Am. 100, 1830–1835.

Boore, D.M., 2003. Simulation of Ground Motion Using the Stochastic Method. Pure Appl. Geophys. 160, 635–676. https://doi.org/10.1007/PL00012553

Boore, D.M., Joyner, W.B., 1984. A note on the use of random vibration theory to predict peak amplitudes of transient signals. Bull. Seismol. Soc. Am. 74, 2035–2039.

Boore, D.M., Thompson, E.M., 2015. Revisions to some parameters used in stochastic-method simulations of ground motion. Bull. Seismol. Soc. Am. 105, 1029–1041.

Bora, S.S., Scherbaum, F., Kuehn, N., Stafford, P., Edwards, B., 2015. Development of a Response Spectral Ground-Motion Prediction Equation (GMPE) for Seismic-Hazard Analysis from Empirical Fourier Spectral and Duration Models. Bull. Seismol. Soc. Am. 105, 2192–2218. https://doi.org/10.1785/0120140297

Cartwright, D.E., Longuet-Higgins, M.S., 1956. The statistical distribution of the maxima of a random function. Proc. R. Soc. Lond. Ser. Math. Phys. Sci. 237, 212–232.

Corotis, R.B., Vanmarcke, E.H., Cornell, A.C., 1972. First passage of nonstationary random processes. J. Eng. Mech. Div. 98, 401–414. https://doi.org/10.1061/JMCEA3.0001591

Kolli, M.K., Bora, S.S., 2021. On the use of duration in random vibration theory (RVT) based ground motion prediction: a comparative study. Bull. Earthq. Eng. 19, 1687–1707. https://doi.org/10.1007/s10518-021-01052-w

Lanzano, G., Luzi, L., Cauzzi, C., Bienkowski, J., Bindi, D., Clinton, J., Cocco, M., D'Amico, M., Douglas, J., Faenza, L., Felicetta, C., Gallovic, F., Giardini, D., Ktenidou, O., Lauciani, V., Manakou, M., Marmureanu, A., Maufroy, E., Michelini, A., Özener, H., Puglia, R., Rupakhety, R., Russo, E., Shahvar, M., Sleeman, R., Theodoulidis, N., 2021. Accessing European Strong-Motion Data: An Update on ORFEUS Coordinated Services. Seismol. Res. Lett. 92, 1642–1658. https://doi.org/10.1785/0220200398

Liu, L., Pezeshk, S., 1999. An improvement on the estimation of pseudoresponse spectral velocity using RVT method. Bull. Seismol. Soc. Am. 89, 1384–1389.

Ou, G.-B., Herrmann, R.B., 1990. Estimation Theory for Peak Ground Motion. Seismol. Res. Lett. 61, 99–107. https://doi.org/10.1785/gssrl.61.2.99

Rupakhety, R., Hernández-Aguirre, V.M., 2026a. Rotation-Invariant Ground-Motion as Directional Selection Operators: A Closed-Form Framework for RotD Response Spectra. https://doi.org/10.31223/X50R1C

Rupakhety, R., Hernández-Aguirre, V.M., 2026b. On the Origin of Directional Variability in Earthquake Response Spectra: A Stochastic Covariance Framework.

Rupakhety, R., Sigbjörnsson, R., 2014. Rotation-invariant mean duration of strong ground motion. Bull. Earthq. Eng. 12, 573–584. https://doi.org/10.1007/s10518-013-9521-9

Rupakhety, R., Sigbjörnsson, R., 2013. Rotation-invariant measures of earthquake response spectra. Bull. Earthq. Eng. 11, 1885–1893. https://doi.org/10.1007/s10518-013-9472-1

Van Houtte, C., Larkin, T., Holden, C., 2018. On durations, peak factors, and Nonstationarity corrections in seismic hazard applications of random vibration theory. Bull. Seismol. Soc. Am. 108, 418–436.

Vanmarcke, E.H., 1976. Structural Response to Earthquakes, in: Developments in Geotechnical Engineering. Elsevier, pp. 287–337. https://doi.org/10.1016/B978-0-444-41494-6.50011-4

Vanmarcke, E.H., 1975. On the Distribution of the First-Passage Time for Normal Stationary Random Processes. J. Appl. Mech. 42, 215–220. https://doi.org/10.1115/1.3423521

Vanmarcke, E.H., Lai, S.-S.P., 1980. Strong-motion duration and RMS amplitude of earthquake records. Bull. Seismol. Soc. Am. 70, 1293–1307.

Wegner, F., 1980. Inverse participation ratio in 2+ε dimensions. Z. Für Phys. B Condens. Matter 36, 209–214. https://doi.org/10.1007/BF01325284